sustainability

Article

Influence of Hydraulic Model Complexity on Results of Water Age and Quality Simulation in Municipal Water Supply Systems

Artur Zajkowski [1,*], Wojciech Kruszyński [1,*], Izabela Bartkowska [1], Łukasz Wysocki [2] and Anna Krysztopik [3]

[1] Department of Water Supply and Sewerage, Bialystok University of Technology, 15-351 Bialystok, Poland
[2] Water Energy Systems (WES), 15-256 Bialystok, Poland
[3] Podlaskie Voivodeship Marshal's Office, 15-888 Białystok, Poland
* Correspondence: artur.zajkowski@doktoranci.pb.edu.pl (A.Z.); w.kruszynski@pb.edu.pl (W.K.); Tel.: +48-571-443-143 (W.K.)

Abstract: The age of water in the municipal water supply system is one of the main factors influencing water quality. To create a good quality hydraulic model, one must achieve a high level of calibration accuracy with real life measurement data. Before we start building our model, we must decide on the model's level of detail, that is, its complexity. We must know if skeletonization of the network graph and different hydraulic timesteps have an influence on simulation results. This study strives to prove that this decision can lead to unforeseen problems during the calibration process, thus making it impossible to achieve the required calibration precision. In order to prove this, two different model variants were created with different levels of graph detail, and simulation data results were used to determine which model variant is best suited to achieve the highest fidelity simulation results. Following this, the chosen model was run with different hydraulic timestep settings, which made it possible to showcase the large influence this setting has on achieved results.

Keywords: hydraulic modeling; GIS; water age; graph complexity; water age; water quality; simulation timestep; result accuracy

check for updates

Citation: Zajkowski, A.; Kruszyński, W.; Bartkowska, I.; Wysocki, Ł.; Krysztopik, A. Influence of Hydraulic Model Complexity on Results of Water Age and Quality Simulation in Municipal Water Supply Systems. *Sustainability* **2022**, *14*, 13701. https://doi.org/10.3390/su142113701

Academic Editors: Gang Liu, Zhisong Chen, Li Gao and Junyu Chen

Received: 2 September 2022
Accepted: 17 October 2022
Published: 22 October 2022

1. Introduction

Scarcity of drinkable water is a growing problem in modern Poland that can be accredited on the one hand to low water retention and on the other hand to many years of poor resource management [1,2]; however, things began to change when Poland aimed to join the European Union. This required country-wide reforms of environmental protection laws, which led to the creation of state organizations such as the Polish Water Organization [3,4].

One of the goals of this organization is to achieve better water management; for example, water companies are required to reduce their water losses and this is forced by financial means [5]. On the other hand, water scarcity can increase the difficulty of supplying water of sufficient quality to end users [6]. One of the tools used in water management is a mathematical hydraulic model [7]. These are integrated into the GIS systems, which allows them to aggregate all types of data on the water distribution network with higher clarity than classical methods [8–12].

The first decision to be made when creating a new hydraulic model of a municipal water supply system is deciding how complex it will be [13,14]. This decision may affect how much time we spend on building and verifying the work of the model and may also affect the costs of its construction [15]. Model complexity can also influence the results of the simulation [16]. Furthermore, during the calibration process, the modeling team has to attain a certain level of calibration accuracy. Otherwise, the model might not be accepted as a proper tool for water system operators [17–20].

Thus, this study aims to prove that model complexity influences simulation results by comparing two models with different levels of graph complexity for the same water supply system. This will allow us to visualize differences in calculated water age which is one of the main factors influencing water quality in the system. A higher precision hydraulic model will allow for better, more accurate, and more precise management of hydraulic and quality conditions in the distribution network. This minimizes costs while maintaining a higher quality of the delivered medium.

The modeling results presented in the article are the result of preliminary research on the issue under consideration. Research will be continued with chosen methodology on real municipal water supply systems. The model will be calibrated based on real data collected in the measurement campaign.

2. Methodology

The study was conducted by creating 2 hydraulic models with varying complexities. The existing hydraulic system was used for modeling purposes. The basis of the model was the water supply system of a city in the Podlasie voivodeship in Poland. The chosen city has around 10,500 inhabitants and has a total pipe length of around 77 km, which supplies water to 10,150 inhabitants. Data for a number of inhabitants comes from the 2010 census. Models were created using the open-source software QGIS 3.24. This allows for creation, visualization, and analysis of geospatial data in a multitude of ways. This software allows for model creation thanks to its rich programing ecosystem written in python programing language, which is ideal for data analysis [21,22].

Following this, geometry and model settings were exported into the simulation software Epanet, created by US EPA. This is considered a leading open-source application for the simulation of municipal water supply systems [23].

After geometry of the network was created, address points were geo-located with use of google geo-localization API. Adress point list standardization was needed before using the API. This allowed for creation of geospatial points with proper localization. Following this, demands were allocated with the Voronoi polygon method, which allowed us to quickly aggregate data to the proper nodes [24,25]. This method allowed us to create polygons, which have a water supply system node ID making it possible to aggregate geo-localized address points to these polygons if they are in their border. Accuracy of this process is highly dependent on the number of nodes in the systems. The total number of polygons is equal to the number of nodes in the model and fills the entire area of the system with polygons without leaving any empty areas. Total demands in both model variants are represented in Table 1. Total water demands were determined with indicators that took into account the number of inhabitants at the water demand point. These demands were divided by type, including single-family housing areas, multi-family housing areas, and industrial areas, which are localized in the eastern and southern areas of the city.

Table 1. Total demands and their types used in both model variants.

Type of Demand	Total Demand $\left[\frac{m^3}{d}\right]$	Number of Demand Points
Single-family housing	1066.00	1923
Multi-family housing	249.98	58
Industry	240.04	1

2.1. Complex Model

The complex model variant includes the whole water supply network, which has 77 km of piping. There are 3792 links and 3736 junctions in total. The average link length is equal to 20.44 m. Thus, almost every water intake point is represented in the model. In the area under study, there is a total of 2192 address points, which were used to allocate nodal water demands. To allocate these demands, we generated a Voronoi polygon grid based on model node geometry, which allowed us to quickly connect both geometrical datasets. On average, there are 1.1 demands allocated to each model node.

Figure 1 is a graphical representation showing the full spatial range of the complex model along with the Voronoi polygon grid. Figure 2 shows the accuracy of demand allocation with the used method.

Figure 1. Spatial representation of hydraulic model extents along Voronoi polygon grid [26].

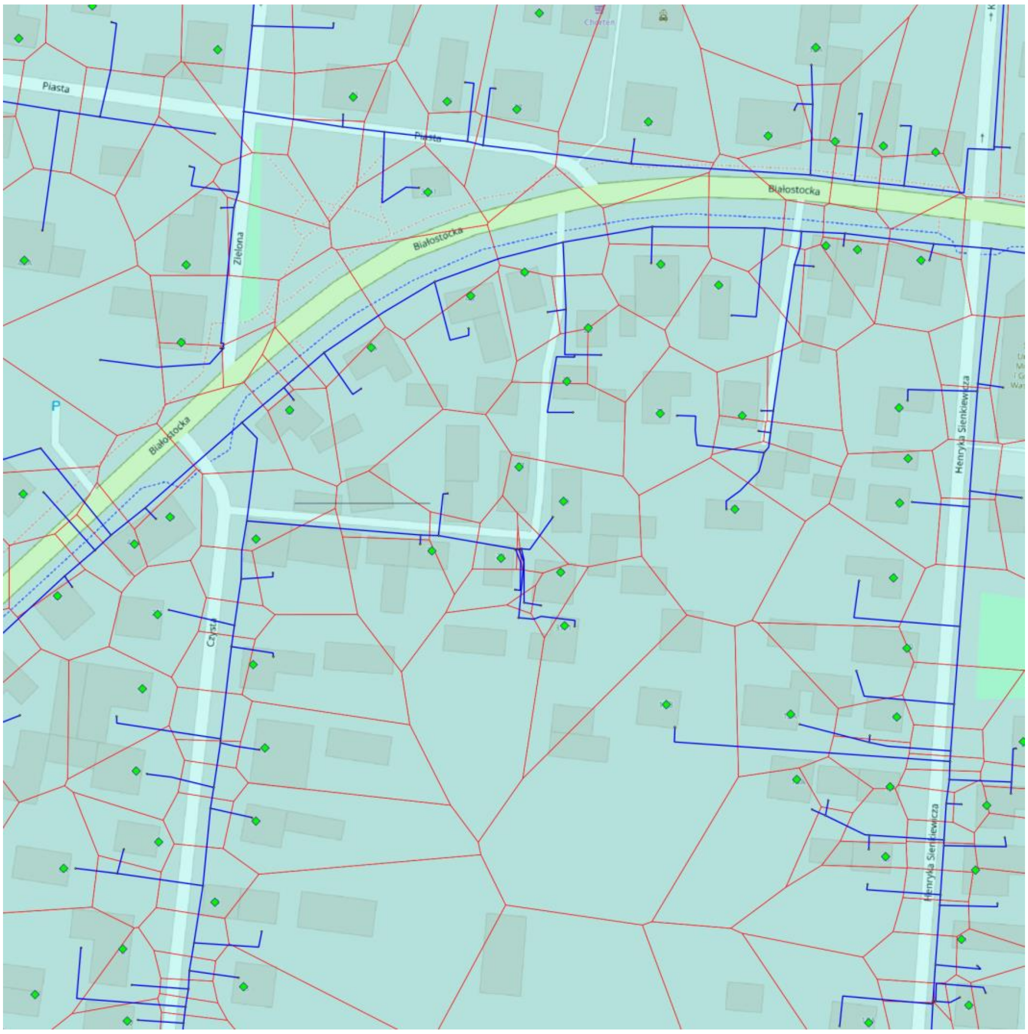

Figure 2. Graphical proof of accuracy of Voronoi polygon method of allocation of nodal demands [26]. Red lines represent borders of Voronoi polygons, water distribution systems is shown as blue lines while green points represent the water demand address points.

2.2. Simplified Model

The simplified model variant includes distribution mains in the network that contains a total of 30.2 km of piping. There are, in total, 136 links and 100 junctions. The amount, number, type, and spatial location of nodal demands are identical to those used in the complex model. In the simplified model, there is a higher per node count of demands allocated, in this case 22.12 compared to 1.1 in the simplified model. The average link length in the simplified model amounts to 222.53 m.

Figure 3 is a graphical representation that shows the full spatial range of the simplified model along with the Voronoi polygon grid. Figure 4 shows the accuracy of demand allocation with the used method. As presented in Figure 1; Figure 2, this method of demand allocation has much lesser accuracy than models with simpler geometries.

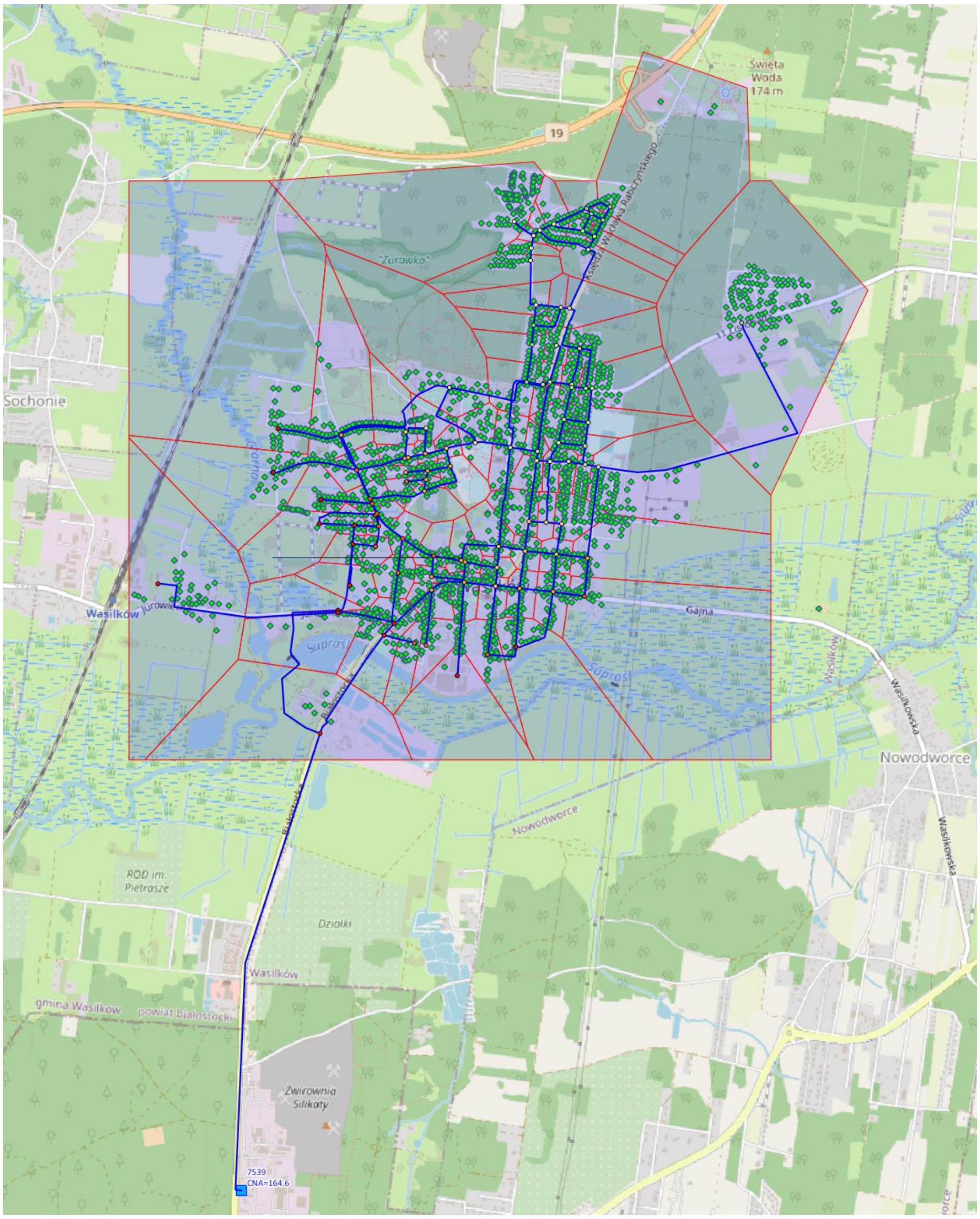

Figure 3. Spatial representation of hydraulic model extents along Voronoi polygon grid [26]. Red lines represent borders of Voronoi polygons, water distribution systems is shown as blue lines while green points represent the water demand address points.

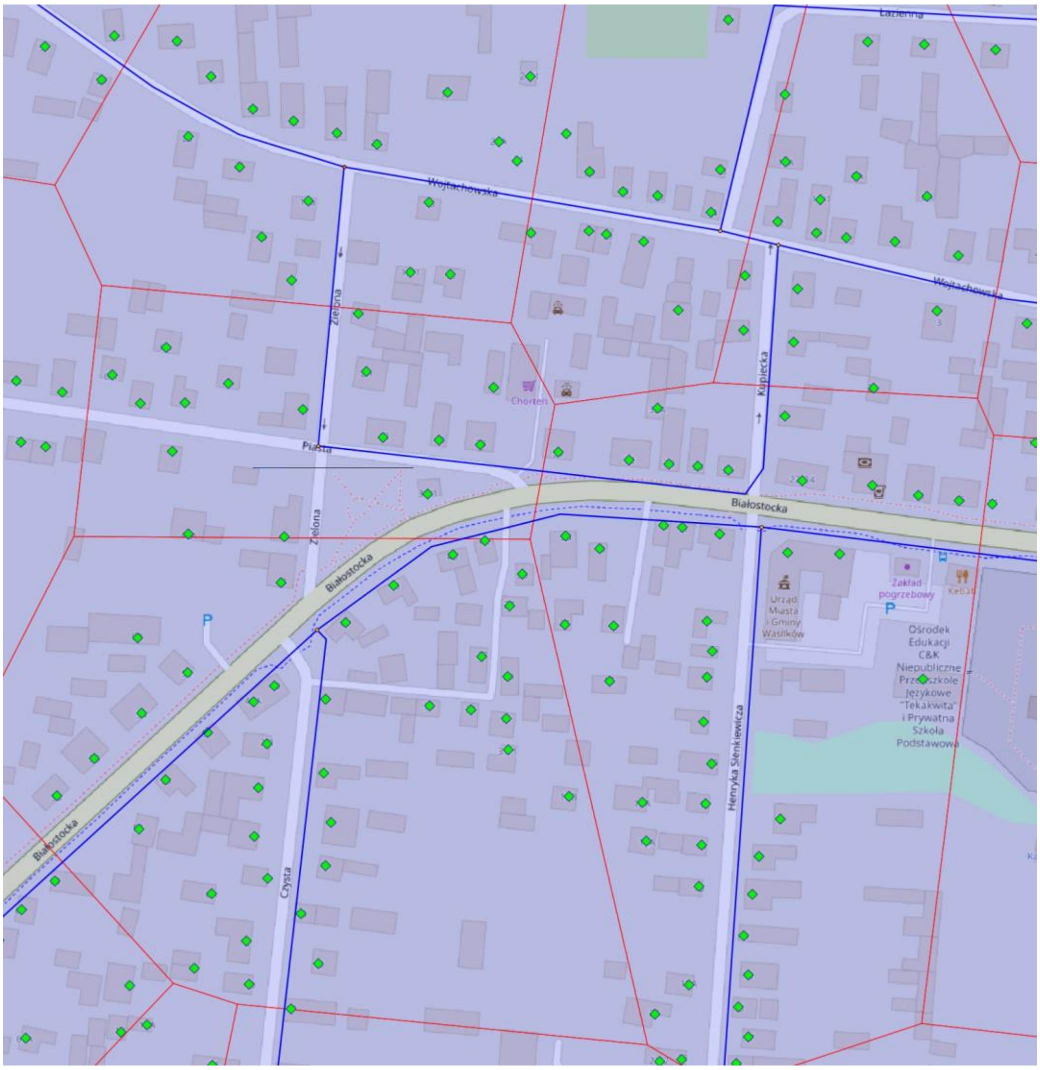

Figure 4. Zoom of hydraulic model that shows how inaccurate the Voronoi polygon method is for simplified model graphs [26]. Red lines represent borders of Voronoi polygons, water distribution systems is shown as blue lines while green points represent the water demand address points.

3. Results

In both models, there are in total 100 junctions that are located at identical coordinates, thus enabling ease of comparison. All comparison nodes were used in the analysis. Models were simulated for 168 h-long demand time series, which equals to seven days of system work from Monday to Sunday. The hydraulic time step was set for 10 min. In total, this gives over 10^5 simulation results for each model variant, hence all results were aggregated to average, median, minimum, and maximum values for each time step.

The main value compared in the analysis is the age of the water in the water system. For simplicity, both datasets were renamed: A represents the simplified model and B represents the complex model.

The plot in Figure 5 shows that the highest density values of water demands in the simplified model variant range from 5 to 10 $\frac{m^3}{d}$, whilst Figure 6 indicates that almost all nodes in the comparative set have close to 0 $\frac{m^3}{d}$ allocated. This means that out of 1556.02 $\frac{m^3}{d}$ of demands for each model variant, only 16.12 $\frac{m^3}{d}$ are allocated at comparative points in the complex model, which is only approximately 1.05% of total demands in the system. This may be one of the main factors influencing the difference in simulation results between both variants.

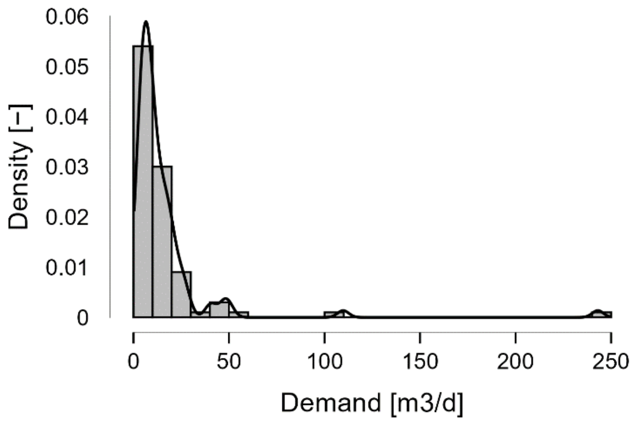

Figure 5. Demand density distribution plot for set of 100 comparative points in simplified model variant—Model A.

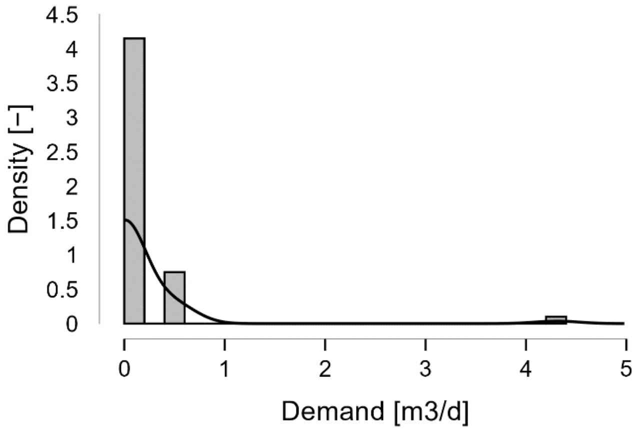

Figure 6. Demand density distribution plot for set of 100 comparative points in complex model variant—Model B.

While comparing data from Figure 7. Comparison of average age values for both model datasets, it can be seen that the average age of water in the system starts to diverge at the ninth hour of simulation and the model's reaction to change in the initial state occurs at almost the same time for both variants. There is a higher correlation in trends between the two models.

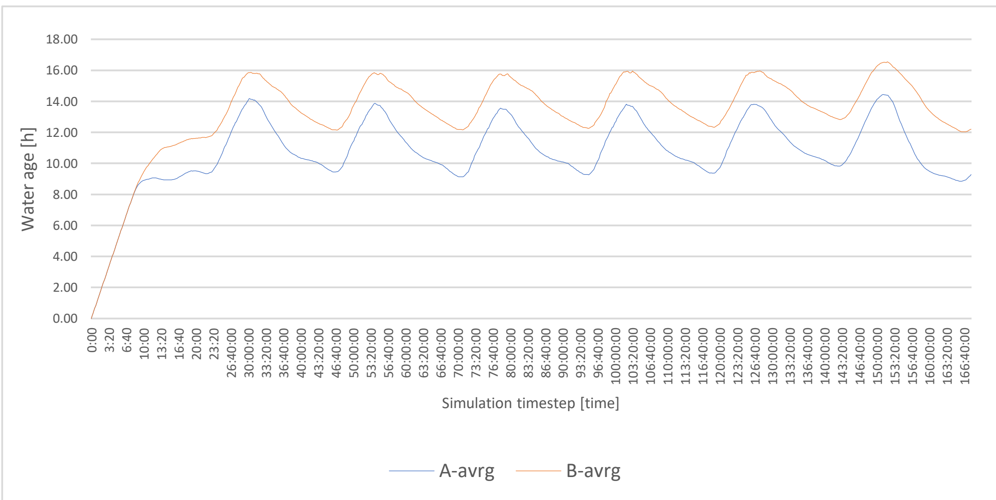

Figure 7. Comparison of average age values for both model datasets.

However, Figure 8 shows that the initial reaction to the change in the model's hydraulic state is different in both models by almost three hours of simulation time. It is also noticeable that both model variants have different median trends for periods of increased water consumption, which is not noticeable in the comparison of average values. This trend difference seems to be occurring in both night and day demand scenarios. This difference will be a very important hindering factor during the calibration step. In a few cases it could prove nigh impossible to meet the required calibration accuracy set up by the client.

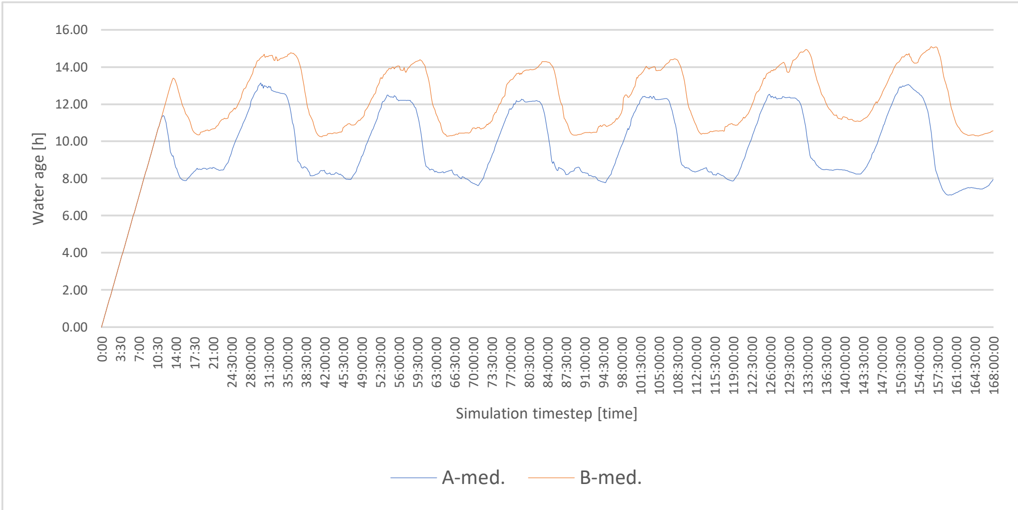

Figure 8. Comparison of median age values for both model datasets.

Nodes with the freshest water or lowest age are mainly those with the highest demand or those that are in the neighborhood of high demand nodes. These nodes can be good indicators for the model difference in a high demand area. The difference is best seen in Figure 9 for high demand times, which are marked by the lowest water age. This difference of 20 min of age on average is by no means a small matter when we consider that these are the most heavily used nodes in the system. The cause of this difference requires more research. One possible reason for this effect is the change of the flow path to nodes caused by the difference in graph density.

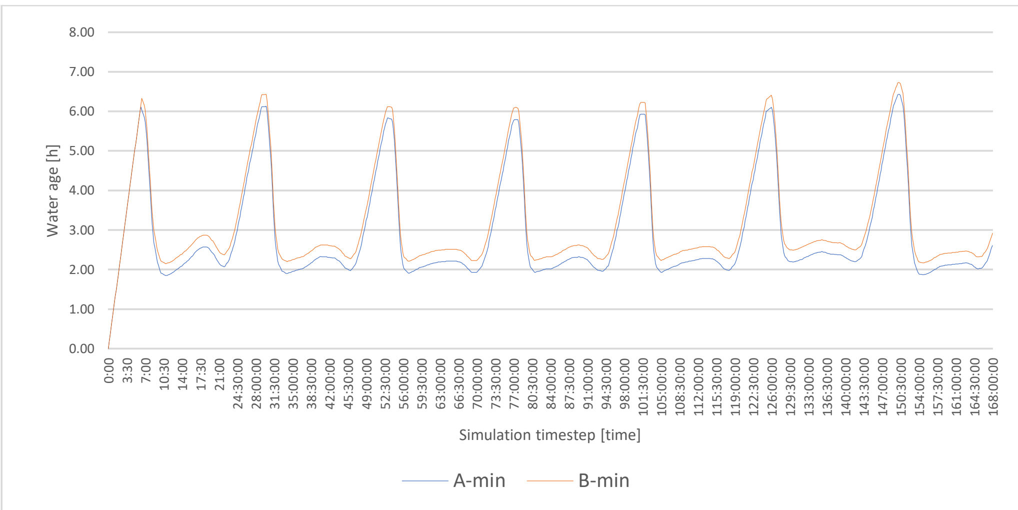

Figure 9. Comparison of minimum age values for both model datasets.

Nodes with the oldest water are those located in desolate parts of the network that have the lowest daily water demand or are on the network peripheries. These parts of the network are always the ones that cause the most problems for operators in maintaining the quality of distributed water in these areas. Figure 10 shows us that between both variants on these network parts there is an almost 35 h difference in the age of water. This is a huge difference when we consider that this almost doubles the age in a simplified model. This level of difference is unacceptable and disqualifies the use of low complexity models for proper approximation of medium age and quality in the system.

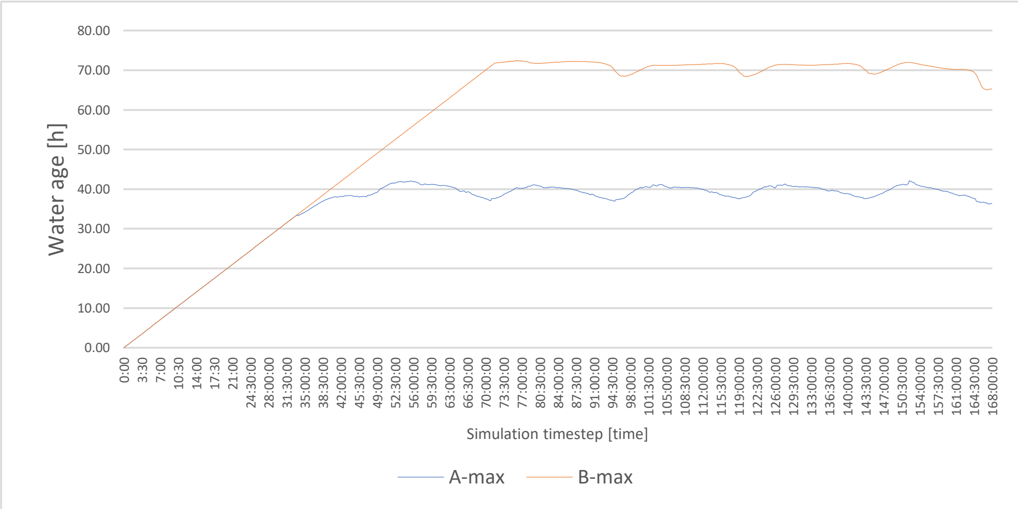

Figure 10. Comparison of maximum age values for both model datasets.

3.1. Descriptive Statistics: Age

Statistical analysis was undertaken with the use of free and open-source software called JASP (Jeffreys's Amazing Statistics Program), which is designed to be easy to use. It allows for easy and quick statistical analysis after a dataset is imported into the software.

As shown in the graphs below, the value ranges of both models are different. The most noticeable difference is visible in Figure 11d, where the age range for model variant A-max is between 35 and 44 h and for model variant B-max it is between 55 and 80 h. The smallest difference is observed in a comparison between the lowest value datasets, where in both variants the age of the water is between 1–1.5 and 7 h.

As shown in Table 2, there is a difference in statistic values for both variants of the model in all datasets. The most noticeable difference is again in the maximum water age dataset, for which mode, median, mean, and standard deviation is almost double in the B model and the smallest difference is in the minimum value datasets. Another noticeable factor is that there is a higher difference between median values of all dataset types than in mean values.

Table 2. Descriptive statistics for both models in all dataset variants.

Descriptive Statistics	A-Avrg	B-Avrg	A-Med	B-Med	A-Min	B-Min	A-Max	B-Max
Valid	1009	1009	1009	1009	1009	1009	1009	1009
Mode	8.940 *	13.500 *	8.490 *	10.420 *	2.210	2.510	40.380	71.270
Median	10.530	13.580	8.750	11.800	2.270	2.570	38.890	69.570
Mean	10.722	13.277	9.524	11.889	2.913	3.202	34.834	55.914
Std. Deviation	2.232	2.641	2.234	2.424	1.306	1.306	10.142	22.039
Skewness	−1.444	−2.426	−0.686	−1.886	1.300	1.276	−2.030	−1.176
Std. Error of Skewness	0.077	0.077	0.077	0.077	0.077	0.077	0.077	0.077
Minimum	0.000	0.000	0.000	0.000	0.000	0.000	0.000	0.000
Maximum	14.440	16.550	13.150	15.100	6.430	6.730	42.120	72.470

* More than one mode exists, only the first is reported.

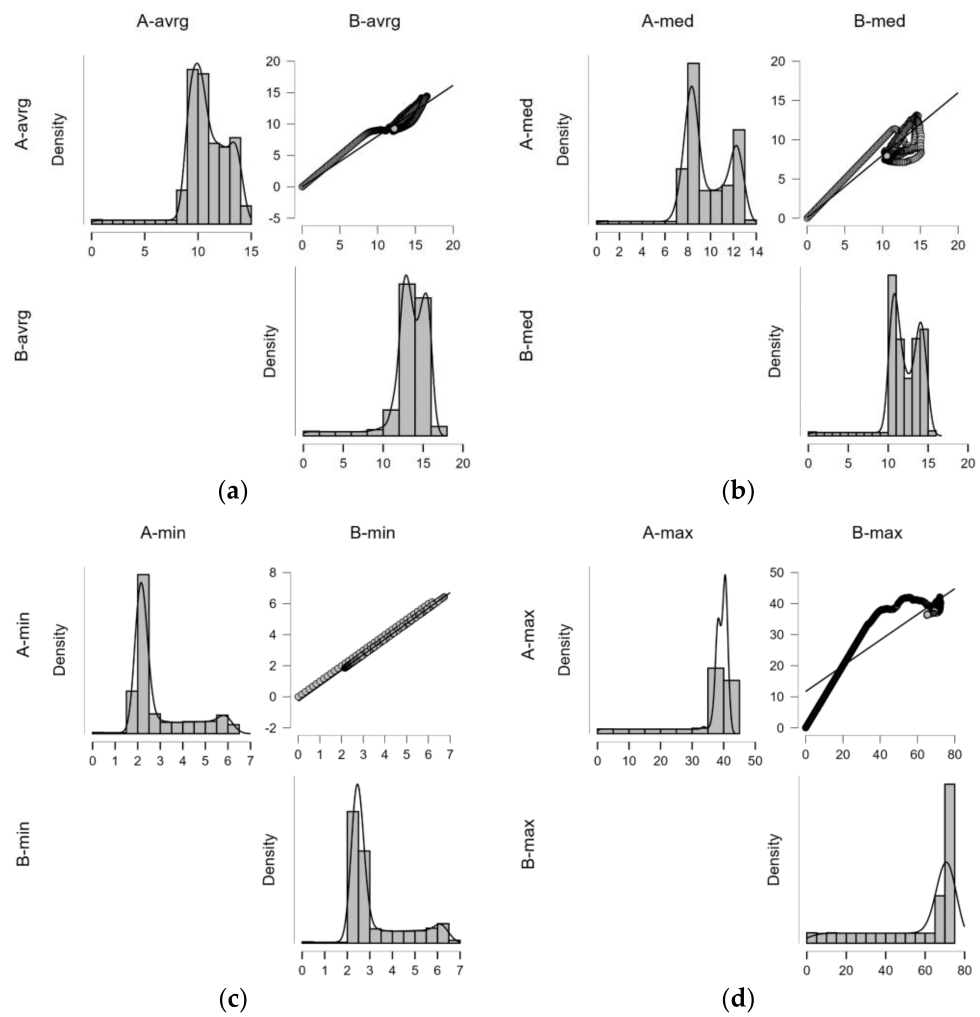

Figure 11. (**a**) Density and correlation plots for average values from both models, (**b**) density and correlation plots for the median values from both models, (**c**) density and correlation plots for minimum values from both models, and (**d**) density and correlation plots for maximum values from both models. X-axes for density graphs represent demand value in $\frac{m^3}{d}$, for correlation plots both x- and y-axes represent values in $\frac{m^3}{d}$.

3.2. Descriptive Statistics Complex Model Full Dataset: Age

An additional statistical analysis was conducted on the full dataset where all nodes in complex model were used. The results are shown in the graphs below—on Figure 12a the density of average age is located between 40 and 50 h, whereas Figure 12b shows that in median density distribution this age is between 37 and 43 h. Figure 12c shows that minimum water age distribution is concentrated at approximately the 1, 2 h mark. Maximum age of water is as shown on Figure 12d is constantly increasing up to the end of the simulation.

3.3. Influence of Simulation Timestep

An additional comparison was made to visualize the influence of the simulation timestep on the quality or age of water results. For this comparison, a complex model was chosen as it has proven to be more accurate in water age or quality approximation. In the model used for the comparison, there are 3736 junctions, from which data were collected. A simulation was run multiple times with identical initial conditions, other than a varying hydraulic timestep value. The basic model was run for 10 min timestep, therefore repeating this was not necessary. There were four different settings chosen, namely 5-, 15-, 20-, and 30-min intervals. Model variants were simulated for a seven-day scenario in the same way as in prior tests. This gives in total over 7.53×10^6 simulation results for the five minute time step model, down to 2.26×10^{-5} for the 30 min timestep simulation results for each variant. Hence a similar method to the earlier approach was used in order to prepare the collected data for analysis. Datasets were aggregated and compared for average, median, minimum, and maximum values for each timestep.

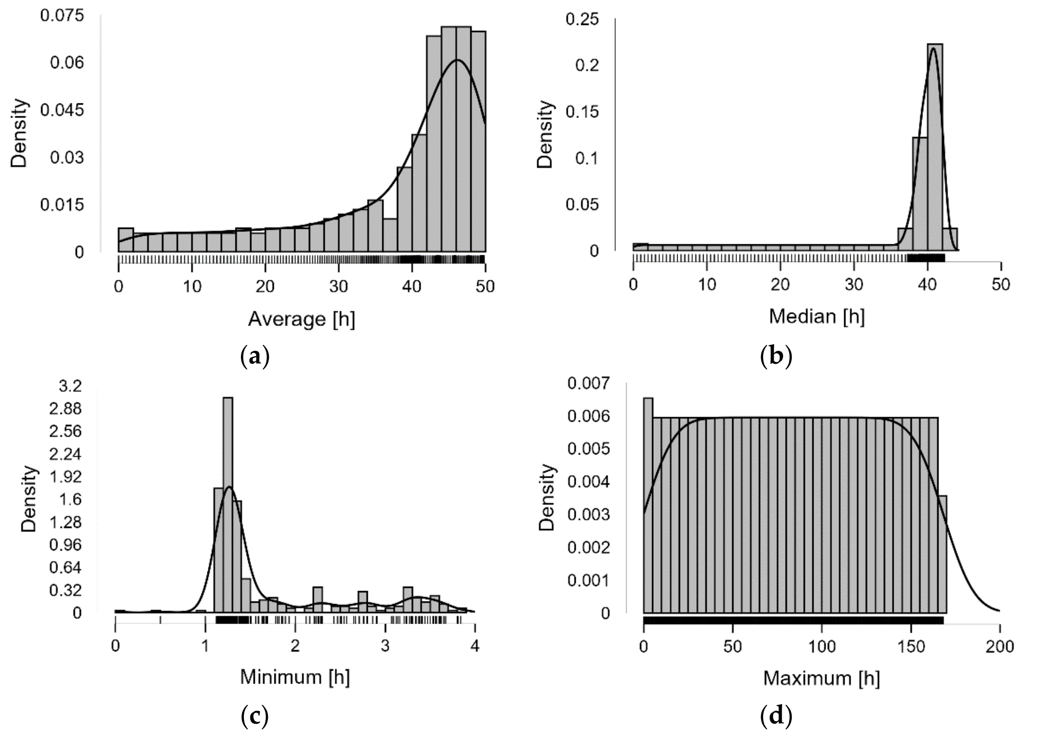

Figure 12. Density graphs for the full dataset of age values for complex model, (**a**) distribution of average age values, (**b**) distribution of median age values, (**c**) distribution of minimum age values, and (**d**) distribution of maximum age values.

This analysis shows a noticeable deviation in calculated results, whereas one would expect a similar simulation result. In Figure 13 it is shown that there is a divergence from the expected trend of values, which means that a longer simulation timestep translates into higher deviation. The same can be seen in the results of the analysis of median values for the age of the water in the system. For this dataset, in Figure 14 it can be seen that in the 15 min timestep model variant there is a noticeable divide between the 5- and 10-min timesteps and the 20- and 30-min timesteps simulation results. One of resulting differences is a change of trend for values in 20- and 30-min timestep model variants. This may be caused by the demand pattern used, but further research is needed. It seems that the optimal timestep for quality simulation is below the 15 min mark.

Comparison of minimum water age data from different model variant simulations indicates that there is a miniscule or close to no difference between different timestep simulation variant results. Minimum age data are compared and represented in Figure 15.

A similar result is achieved in the comparison of maximum water age data resulting from the simulation of varying timestep settings. This comparison indicates that water age simulation results are identical for all variants. Maximum age data are compared and represented in Figure 16.

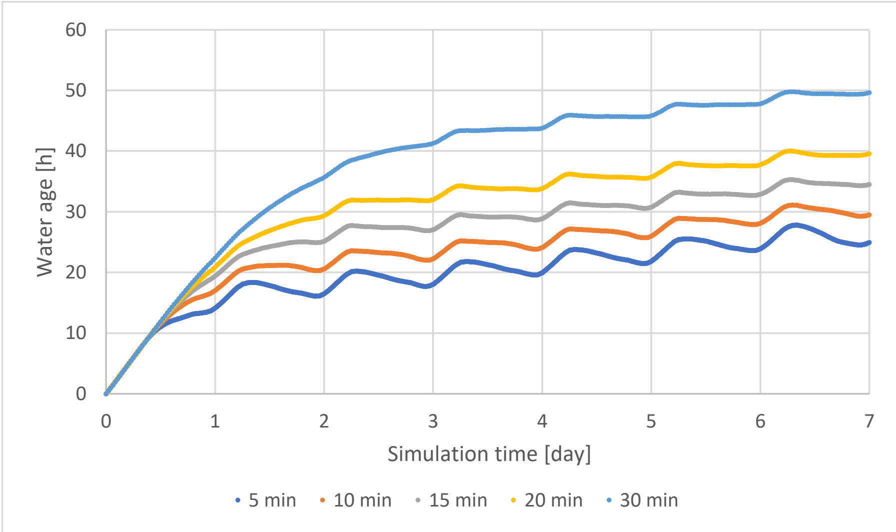

Figure 13. Comparison of average age values for all model variant datasets.

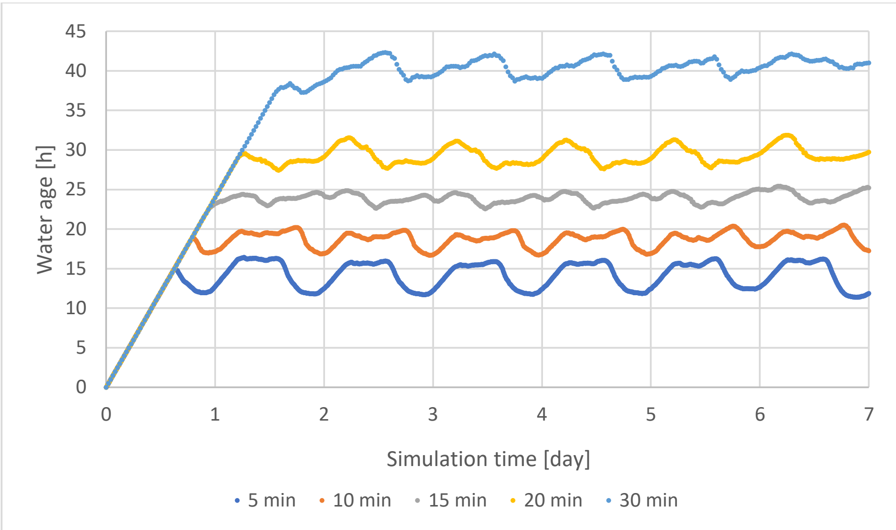

Figure 14. Comparison of median age values for all model variant datasets.

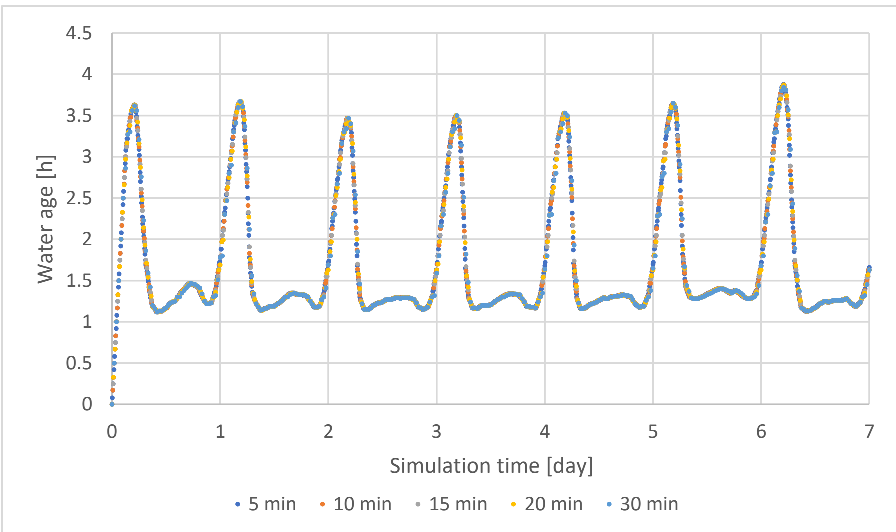

Figure 15. Comparison of minimum age values for all model variant datasets.

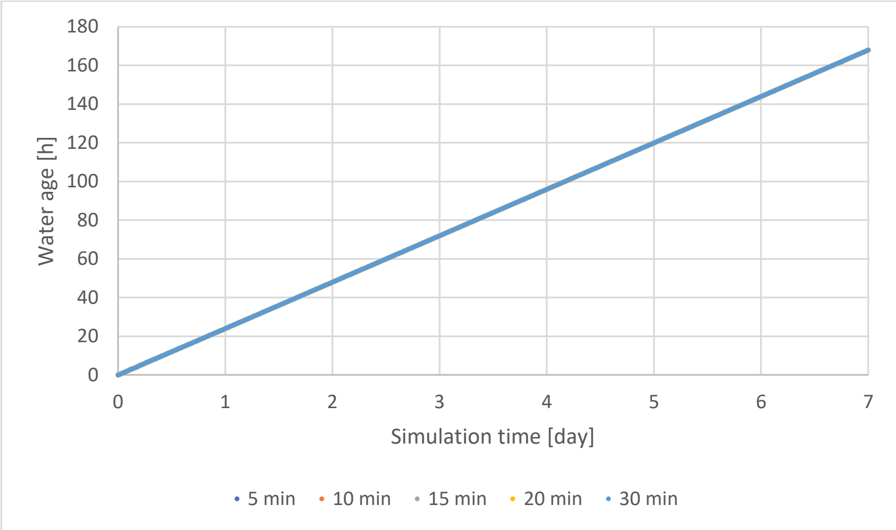

Figure 16. Comparison of maximum age values for all model variant datasets.

3.4. Descriptive Statistics: Influence of Results due to Timestep

After data obtained from the simulation were inputted into the statistical software, a descriptive statistical analysis was undertaken in the same way as in the previous case. Results are shown below.

In Table 3 it can be seen that results are divided mainly into two groups—one below the 15 min range (highly corelated) and one above the 15 min mark, which is the initial point of big result deviation in the case of this test.

Table 3. Descriptive statistics for full dataset of complex model age values.

Descriptive Statistics	Average	Median	Minimum	Maximum
Valid	337	337	337	337
Missing	0	0	0	0
Mode [a]	0.000	39.130	1.300	0.000
Median	43.482	39.965	1.310	84.000
Mean	38.092	35.475	1.712	84.000
Std. Deviation	12.743	10.489	0.787	48.714
Skewness	−1.417	−2.021	1.373	4.155×10^{-20}
Std. Error of Skewness	0.133	0.133	0.133	0.133
Minimum	0.000	0.000	0.000	0.000
Maximum	49.819	42.335	3.840	168.000

[a] More than one mode exists, only the first is reported.

Table 4 show that average, median minimum and maximum statistical values are equal for models of both 20 and 30 min timestep interval variants. Differences in values begin to manifest in model variants with 5 10 and 15 min timesteps.

Table 4. Descriptive statistics for both models in all dataset variants.

Descriptive Statistics		Mode	Median	Mean	Std. Deviation	Skewness	Std. Error of Skewness	Minimum	Maximum
Average	5 min	0.000	20.472	19.805	5.474	−1.225	0.055	0.000	27.863
	10 min	0.000	24.689	23.261	6.434	−1.507	0.077	0.000	31.148
	15 min	27.449	29.16	26.992	7.721	−1.62	0.094	0.000	35.321
	20 min	0.000	33.831	30.79	9.263	−1.602	0.109	0.000	40.061
	30 min	0.000	43.482	38.092	12.743	−1.417	0.133	0.000	49.819

Table 4. *Cont.*

Descriptive Statistics		Mode	Median	Mean	Std. Deviation	Skewness	Std. Error of Skewness	Minimum	Maximum
Median	5 min	15.690	14.09	13.587	2.788	−2.204	0.055	0.000	16.44
	10 min	19.500	18.85	17.691	3.596	−3.131	0.077	0.000	20.52
	15 min	23.875	23.81	22.242	5.01	−2.922	0.094	0.000	25.455
	20 min	0.000	33.831	30.79	9.263	−1.602	0.109	0.000	40.061
	30 min	0.000	43.482	38.092	12.743	−1.417	0.133	0.000	49.819
Min	5 min	1.290	1.32	1.713	0.782	1.396	0.055	0.000	3.88
	10 min	1.290	1.32	1.713	0.783	1.391	0.077	0.000	3.87
	15 min	1.280	1.31	1.713	0.784	1.387	0.094	0.000	3.86
	20 min	0.000	33.831	30.79	9.263	−1.602	0.109	0.000	40.061
	30 min	0.000	43.482	38.092	12.743	−1.417	0.133	0.000	49.819
Max	5 min	5.180	84	84.005	48.525	4.122×10^{-4}	0.055	0.000	168
	10 min	0.000	84	84.001	48.567	1.156×10^{-4}	0.077	0.000	168
	15 min	0.000	84	84.001	48.604	9.511×10^{-5}	0.094	0.000	168
	20 min	0.000	33.831	30.79	9.263	−1.602	0.109	0.000	40.061
	30 min	0.000	43.482	38.092	12.743	−1.417	0.133	0.000	49.819

4. Discussion

More complex models can be used in a wider range of possible technical applications. For example, as Zimoch and Bartkiewicz [6] stated, hydraulic models can be helpful for a wide range of jobs related to management of water age in the system or in planning sysem-wide flushing operations. A higher complexity model is a tool that enables users to properly plan the best flushing route and calculate water volume lost due to such an operation. In a low complexity model, some fidelity is always lost due to geometry simplification.

As Guth and Klingel have stated, it is possible to achieve high accuracy of demand distribution in a model with the use of Voronoi polygons [27]. However, one cannot forget to apply the proper model complexity before applying this method; even if it is possible to very accurately localize each demand to proper node differences surfacing in simulation results [28,29], simulation results can vary up to 100% and possibly more due to the difference in model structure and graph density.

This can be attributed to the difference in nodal demand allocation, demand aggregation, and fewer routes that water can pass through in the model. It seems to increase in peripheral parts of the network, where base demands are lower in amount and density across the nodes.

Abhijith et al. [30] have proven that it is indeed possible to simulate things such as bacterial regrowth and THM formations in water distribution systems. This could be achieved by more complex iteration of EPANET software. In the case where water age is one of the key points for quality simulation, one must decide on model complexity due to the fact that it influences simulation results.

An increase in the maximum values of water age in the complex model variant can be attributed to the fact that in complex networks of the model there will be some nodes and links that have close to zero nodal demands allocated.

5. Conclusions

In the process of model calibration, one should focus more on using average values, because using median values can change the trend depending on model complexity during the different parts of each simulation day. This would influence model quality while comparing real life measurement data with model results, lowering the model quality score. This, in some cases, can invalidate calibration results.

The hydraulic models can be used by water supply companies to assess water age in the system, allowing them to more accurately set the required chlorine amount during the chlorination process. Having a model which has an inherent error of up to 100% in the water age, due to its complexity, can lead to serious consequences, such as the increased presence of trihalomethanes, which can cause cancer in people who come into contact with this chemical compound. Another problem that can arise with incorrect system workflow due to small model complexity is that this difference can be critical to correct the approach of system optimizations and planning of system-wide flushing operations.

Hence, it is critical that the user tasked with the job of analyzing the water quality, or another task that is connected with the quality analysis, remembers that there are a few seemingly hidden but very important factors which determine the simulation results. The first factor is model complexity; essentially, the more complex the model the better. The second factor is the quality timestep that can be adjusted after the model building stage. The third factor is the used demand pattern timestep, which seems to be one of the causes of divergence in results of simulation of varying timestep models.

In conclusion, theoretical model results indicate that the used method will be innovative, and it will affect the results of modelling. Results of using this method in tandem with real data calibration will be utilized in further studies.

Author Contributions: Conceptualization, W.K. and A.Z.; methodology, A.Z. and A.K.; validation, I.B. and Ł.W.; formal analysis, I.B. and A.Z.; writing—original draft preparation, review, and editing, A.Z., Ł.W. and W.K. All authors have read and agreed to the published version of the manuscript.

Funding: The research was carried out as part of the work No. WZ/WB-IIŚ/3/2022 in Bialystok University of Technology and financed from funds for education of the Ministry of Science and Higher Education.

Institutional Review Board Statement: Not applicable.

Informed Consent Statement: Not applicable.

Data Availability Statement: Not applicable.

Conflicts of Interest: The authors declare no conflict of interest.

References

1. Gwoździej-Mazur, J.; Świętochowski, K. Analysis of the water meter management of the urban-rural water supply system. *E3S Web Conf.* **2018**, *44*, 00051. [CrossRef]
2. Malmur, R.; Mrowiec, M.; Ociepa, E.; Deska, I. Sustainable Water Management in Cities Under Climat Changes. *Probl. Ekorozw.* **2018**, *13*, 133–138.
3. Dzienis, L.; Lebiedowski, M. *Water Supply and Water Treatment Systems in Agricultural and Industrial Regions: Selected Problems*; HARD: Olsztyn, Poland, 2009.
4. Denczew, S. *Podstawy Modelowania Systemów Eksploatacji Wodociągów I Kanalizacji: Teoria I Praktyka*; Polska Akademia Nauk. Komitet Inżynierii Środowiska: Lublin, Poland, 2006. (In Polish)
5. Gwoździej-Mazur, J.; Świętochowski, K. Evaluation of Real Water Losses and the Failure of Urban-Rural Water Supply System. *J. Ecol. Eng.* **2021**, *22*, 132–138. [CrossRef]
6. Zimoch, I.; Bartkiewicz, E. Modeling of water age as an element supporting the management of the water supply system. *Proc. ECOpole* **2018**, *12*, 611–620. [CrossRef]
7. Wilson, A.I. Hydraulic Engineering and Water Supply. In *The Oxford Handbook of Engineering and Technology in the Classical World*; Oxford University Press: Oxford, UK, 2009. [CrossRef]
8. Trębicka, A. A Model of Time Variability of Characteristic Parameters of the Water Distribution System as a Base of Information and the Basis of Mathematical Modelling. *J. Ecol. Eng.* **2020**, *21*, 46–51. [CrossRef]
9. Sitzenfrei, R.; Möderl, M.; Rauch, W. Automatic generation of water distribution systems based on GIS data. *Environ. Model. Softw.* **2013**, *47*, 138–147. [CrossRef]
10. Brenna, L.; Dyrkoren, P.; Vangdal, A.; Poulton, M.; Bruaset, S. Report on System Development, Method Applicability, and Pipeline Condition Data for Modelling Purposes. 2014. Available online: http://hdl.handle.net/10251/35740 (accessed on 2 February 2022).
11. National Research Council. *Drinking Water Distribution Systems: Assessing and Reducing Risks*; National Academies Press: Washington, DC, USA, 2007. Available online: https://nap.nationalacademies.org/catalog/11728/drinking-water-distribution-systems-assessing-and-reducing-risks (accessed on 8 March 2022).
12. Kulbik, M. *Komputerowa Symulacja i Badania Terenowe Miejskich Systemów Wodociągowych*; Monografie 49; Politechnika Gdańska: Gdańsk, Poland, 2004. (In Polish)
13. Trębicka, A. Efficiency End Optimum Decisions in the Modeling Process of Water Distribution. *J. Ecol. Eng.* **2018**, *19*, 254–258. [CrossRef]

14. Gwoździej-Mazur, J.; Andraka, D.; Kaźmierczak, B.; Kruszyński, W. On-Line Water Consumption Monitoring as a Tool for Optimal Management of Water Distribution Network. *Environ. Sci. Proc.* **2021**, *9*, 26. [CrossRef]
15. Haestad, M.; Walski, T.; Chase, D.V.; Savic, D. *Advanced Water Distribution Modeling and Management*; Bentley Institute Press: Waterbury, CT, USA, 2004.
16. Gwoździej-Mazur, J.; Świętochowski, K. Non-Uniformity of Water Demands in a Rural Water Supply System. *J. Ecol. Eng.* **2019**, *20*, 245–251. [CrossRef]
17. Boulos, P.F. *Comprehensive Water Distribution Systems Analysis Handbook for Engineers and Planners*; American Water Works Association: Washington, DC, USA, 2004.
18. Studzinski, J. ICS System Supporting the Water Networks Management by Means of Mathematical Modelling and Optimization Algorithms. *J. Autom. Mob. Robot. Intell. Syst.* **2015**, *9*, 48–54. [CrossRef]
19. Clarke, R. Modeling Water Quality in Distribution Systems, 2nd ed.; American Water Works Association Washington DC, USA: 2011. Available online: https://ebookcentral-proquest-com.bazy.pb.edu.pl/lib/bialostocka/reader.action?docID=3116755 (accessed on 10 February 2022).
20. Denczew, S.; Królikowski, A. *Podstawy Nowoczesnej Eksploatacji Układów Wodociągowych i Kanalizacyjnych*; Arkady: Warsaw, Poland, 2002. (In Polish)
21. Wu, Z.Y.; Boulos, P.F.; Orr, C.H.; Ro, J.J. An Efficient Genetic Algorithm Approach to an Intelligent Decision Support System for Water Distribution Networks. In Proceedings of the 4th International HydroInformatics Conference, Iowa Institute of Hydraulic Research, Iowa City, IA, USA, 23–27 July 2000.
22. Vairavamoorthy, K.; Yan, J.; Galgale, H.M.; Gorantiwar, S.D. IRA-WDS: A GIS-based risk analysis tool for water distribution systems. *Environ. Model. Softw.* **2007**, *22*, 951–965. [CrossRef]
23. Lewis, A. Rossman and others. In *EPANET 2.2 User Manual*; U.S. Environmental Protection Agency: Washington, DC, USA, 2020. Available online: https://epanet22.readthedocs.io/_/downloads/en/latest/pdf/ (accessed on 1 February 2022).
24. Aurenhammer, F.C.D. Voronoi Diagrams—A Survey of a Fundamental Geometric Data Structure. *ACM Comput. Surv.* **1991**, *23*, 345–405. [CrossRef]
25. Okabe, A.; Satoh, T.; Furuta, T.; Suzuki, A.; Okano, K. Generalized net-work Voronoi diagrams: Concepts, computational methods, and applications. *Int. J. Geogr. Inf. Sci.* **2008**, *22*, 965–994. [CrossRef]
26. Kruszyński, W.; Zajkowski, A. Influence of Level of Detail (LOD) in Hydraulic Model Geometry with Demand Allocation by Voronoi Polygon Method on Chosen Parameters. *Environ. Sci. Proc.* **2021**, *9*, 35. [CrossRef]
27. Guth, N.; Klingel, P. Demand Allocation in Water Distribution Network Modelling—A GIS-Based Approach Using Voronoi Diagrams with Constraints. In *Application of Geographic Information Systems*; IntechOpen Limited: London, UK, 31 October 2012. [CrossRef]
28. McKenzie, R.; Wegelin, W. Implementation of pressure management in municipal water supply systems. In Proceedings of the EYDAP Conference "Water: The Day After", Athens, Greece, 6–8 November 2009; Volume 20. Available online: https://www.miya-water.com/fotos/artigos/03_implementation_of_pressure_management_in_municipal_water_supply_systems_3323280065a328bc009ead.pdf (accessed on 5 February 2022).
29. Baader, J.; Fallis, P.; Hübschen, K.; Klingel, P.; Knobloch, A.; Laures, C.; Oertlé, E.; Trujillo Alvarez, R.; Ziegler, D. Guidelines for Water Loss Reduction—A Focus on Pressure Management. 2011. Available online: https://www.researchgate.net/publication/318792810_Guidelines_for_water_loss_reduction_-_a_focus_on_pressure_management (accessed on 7 February 2022).
30. Abhijith, G.R.; Kadinski, L.; Ostfeld, A. Modeling Bacterial Regrowth and Trihalomethane Formation in Water Distribution Systems. *Water* **2021**, *13*, 463. [CrossRef]